Cement and Concrete Research 42 (2012) 593–597

Contents lists available at SciVerse ScienceDirect

Cement and Concrete Research

journal homepage: http://ees.elsevier.com/CEMCON/default.asp

Hydration of C_3S thin films

Vanessa Rheinheimer, Ignasi Casanova *

Department of Construction Engineering and Center for Research in Nanoengineering, Universitat Politècnica de Catalunya, Barcelona Tech. Campus Nord, B1-109C, 08034 Barcelona, Spain

ARTICLE INFO

Article history:
Received 19 September 2011
Accepted 26 January 2012

Keywords:
Tricalcium silicate (D)
Thin film
X-ray photoelectron spectroscopy
Calcium silicate hydrate (B)

ABSTRACT

Thin films of C_3S of a few tens of nanometers were produced by electron beam evaporation. After verification that the chemical composition of the bulk material remained unchanged, the samples were hydrated with water vapor in a reaction chamber under saturated pressure and temperature conditions, and were kept isolated from atmospheric exposure throughout the whole duration of the experiment. Analyses by X-ray photoelectron spectroscopy at different stages of hydration evidence a shift of the Si peaks to higher energies and a subsequent decrease of the Ca–Si binding energy distance, indicating silicate polymerization expected upon formation of C–S–H. The measured molar Ca/Si ratio evolves from that of a jennite-like material, of about 1.55, at the beginning of the experiment (attributed to pre-hydration of the thin films), to a tobermorite-like ratio of 0.85 after 3 h of hydration.

1. Introduction

It is commonly agreed that cement reacts with water through a dissolution–precipitation process. This occurs when the ions in the solution eventually coalesce and lead to hydration products that, having a lower solubility than the anhydrous phases, precipitate and form a stiff paste. The properties, kinetic evolution and hardening of such material, grossly depend on the thermodynamic properties of its individual constituents. Despite this, C_3S is the major clinker phase in Portland cement, and hence a very important component to fully understand and predict the development of strength and durability of concrete. However, the details of its hydration mechanisms are not fully understood, and important gaps remain on the nature of the induction period and hydration kinetics.

Hydration kinetics depends on many factors such as the initial concentration and chemical evolution of the solution, temperature, dissolution and precipitation rates, and interface area between solid and solution, among others [1–4]. Tricalcium silicate reaction with water undergoes a slow down after initial contact, the so-called induction or dormant period, followed by a rapid increase of the rate of hydration. The many theories about the nature of this phenomenon have been recently summarized and discussed by Juilland et al. [3]. However, the calcium silicate hydrates form preferentially on a smooth or pitted surface by isolated clumps and require extra energy for the formation of the first pit. The precipitation of C–S–H seems to happen at crystal defect sites [5], although nucleation of silicate hydrates by reaction of pure C_3S with water is difficult to monitor since it happens very fast due to the high supersaturation [4]. Furthermore, the presence of impurities yields to a different grain growth behavior when compared with pure, stoichiometric C_3S. This is probably due to differences in the density of reactive sites and thus, affects the hydration kinetics [2].

The first attempts to understand the surface chemistry of early hydration of tricalcium silicate included X-ray photoelectron spectroscopy (XPS) investigations that evidenced that the Ca 2p/Si 2p ratio must be lower in hydrated samples than in anhydrous C_3S, and that the Si binding energies and peak shape of the hydrated particles show significant changes shortly after the onset of hydration [6]. As hydration progresses, the Ca/Si ratio of C_3S pastes has been observed to decrease to values between 1.5 and 1.8 by several authors [7–9].

At macroscale, C–S–H is essentially an amorphous material. However, it has a short-range nanocrystalline structure. It has been recently suggested that, at the nanoscale, C–S–H is granular in nature [4]. Previous investigations have proposed that growth of hydrates takes place in different spots by the addition of silicate tetrahedra and development of silicate sheets incorporating calcium and hydroxyl in the interlayers [10], and that the formation of independent C–S–H nanoparticles stimulates the nucleation of new ones on their surfaces [11]. Also, atomistic simulations and modeling approaches have been developed with the aim of better understanding the process [12–17], suggesting on one hand that the C–S–H density is not uniform and it decreases with distance from the alite grain surface and, on the other, that dimeric silicates are formed just after the end of the dormant period.

In this work, we show the results of the chemical evolution upon hydration of C_3S thin films produced by electron-beam evaporation of powdered raw material. In situ hydration of the thin films and continuous monitoring of their chemical and microstructural evolution by XPS and focused ion beam (FIB) sectioning and imaging shed

* Corresponding author at: Center for Research in Nanoengineering (CRnE), C/Pascual i Vila, 15. 08028 Barcelona, Spain. Tel.: +34 934015794; fax: +34 934134033.
E-mail address: ignasi.casanova@upc.edu (I. Casanova).

0008-8846/$ – see front matter © 2012 Elsevier Ltd. All rights reserved.
doi:10.1016/j.cemconres.2012.01.002

Table 1
XPS analytical conditions and chemical compositions of starting material and thin films.

Region	XPS conditions			Composition	
	Start energy (eV)	End energy (eV)	Dwell time (ms)	Starting material (at.%)	Thin film (at.%)
Wide	0	1200	0.1	–	–
C 1s	275	295	0.5	22.2	20.7
O 1s	525	540	1	54.6	55.4
Ca 2p	339	359	1	18.1	17.8
Si 2s	143	163	1	5.1	6.1
Si 2p	94	114	1		
Total	–	–	–	100	100

some additional light on the complex problem of the hydration mechanisms of cementitious materials.

2. Experimental

Thin films of C_3S were produced by electron beam bombardment of a powder target, and the sputtered/evaporated material was collected onto a silicon wafer in a high-vacuum chamber. The thin film production procedure and verification of the preservation of the chemical and mineralogical composition have been described elsewhere [18]. For this study, films of about 110 nm in thickness were produced and kept in an inert N_2 atmosphere in order to minimize atmospheric pre-hydration and carbonation prior to the beginning of the hydration experiments.

Samples of the thin films were fixed in a holder with an adhesive-backed copper tape and their chemical composition was verified with the XPS system at UPC's Center for Research in Nanoengineering, equipped with an Al anode XR50 source operating at 150 W and a Phoibos MCD-9 detector. Spectra were recorded with a pass energy of 25 eV at 0.1 eV/step, and pressure below 10^{-9} mbar. A flood gun (0.36 eV, 0.24 mA) was used to avoid sample charging. The angle between the sample and the emission gun was settled at 15º and their distance to 30 mm. For each pattern, general scans were repeated three times and specific high resolution scans were carried out for Ca, Si, C and O (Table 1).

After running the initial pattern, dry thin film samples were transferred individually to a reaction chamber in the same vacuum line as the XPS, thus avoiding any atmospheric contamination. Prior to hydration, the system was purged for 5 min with an Ar flux of 20 mL/min.

Spectra were treated with CasaXPS software. A Shirley background was assumed in all cases. Spectra were corrected for charging effects using the adventitious carbon peak at 284.8 eV.

A Focused Ion Beam/Scanning electron microscope system (FIB/SEM) (Zeiss Neon 40) was used for observation and selective milling of samples, both unreacted and exposed to water vapor for 182 min. The equipment is a Galium FIB with 1 pA − 50 nA, 2–30 kV and 7 nm resolution, and the SEM (Shottky FE) with a 4 pA–20 nA, 0.1–30 kV, and 1.1 nm resolution depending on the sample. A gas injection system was used for selective milling and deposition of platinum to avoid ion beam defocussing.

3. Results and discussion

XPS analyses show a drift, after 3 h of exposure to water vapor, of the main Si 2p (101.9 to 102.6 eV) and Si 2s (152.9 to 153.4 eV) peaks. These are positioned at lower energies than those previously reported (100.57 eV for Si 2p in fresh C_3S, [19]). The Si peaks display a shift to higher energies and slight broadening (e.g. average FWHM of 3.3 *vs.* 2.5 eV in the 152.9–153.4 and 101.9–102.6 eV ranges, respectively; Fig. 1 and Table 3), indicating the progressive disordering of the silicate structure related to C–S–H formation.

The Ca binding energies show a somehow more erratic behavior, but no progressive shift has been observed, as in the case of Si, when hydration goes on (Fig. 2). The Ca $2p_{3/2}$ peak is centered at 347.1 eV (Table 3) for fresh C_3S, a value slightly lower than the one previously reported by Black et al. [19] (346.55 eV). Measuring the energy separation between Ca $2p_{3/2}$ and Si 2p peaks ($\delta_{Ca2p-Si2p}$) provides information about hydration.

During the hydration process the Si peaks shift to higher energies, while the Ca peaks stay in the same binding energy, and any changes are mainly due to the broadening and the contribution from carbonates and silicates. Prior to analysis all spectra were corrected for charging effects using the adventitious carbon peak at 284.8 eV and the same background (Shirley) was used. This approach avoids errors due to charge correction [6,20]. The calculated Ca–Si distances and their evolution with time of hydration are plotted in Fig. 3. The initial values of $\delta_{Ca2p-Si2p}$ found in this work (245.3 eV) are somewhat lower than those reported by Regourd et al. [6] (245.7 eV), Long et al. [21] (245.95 eV) and Black et al. [22] (245.99 eV). As discussed above,

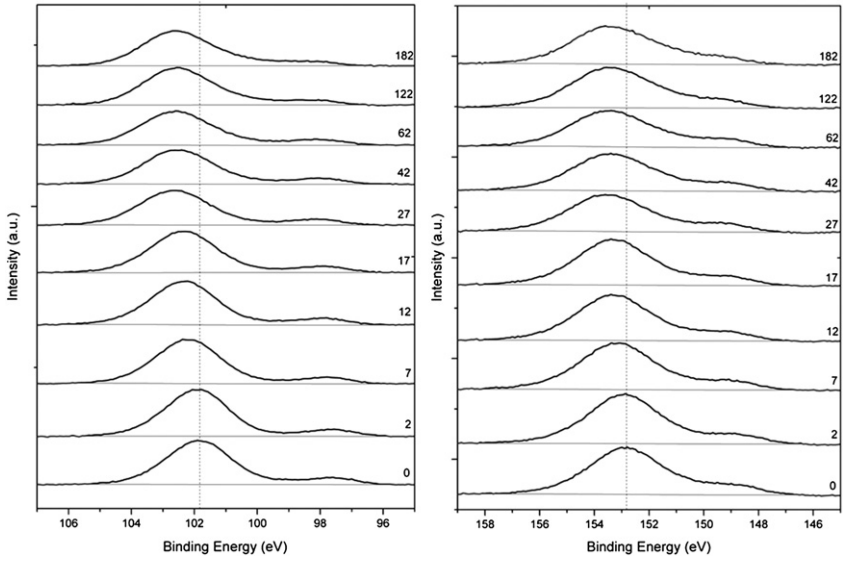

Fig. 1. XPS spectra of the C_3S thin film showing the evolution of the Si 2p (left) and 2s (right) peaks during exposure to water vapor. Labels on the right indicate time of hydration in minutes.

Table 2
Experiment conditions for each stage of hydration of thin films.

Time (min)	Accumulated time (min)	Temperature (°C)	P (H_2O) (mbar)
2	2	28.8	39.59
5	7	27.9	37.58
5	12	28.0	37.79
5	17	28.4	38.68
10	27	26.6	34.82
15	42	26.9	35.44
20	62	26.6	34.82
60	122	26.7	35.03
60	182	27.4	36.49

Table 3
Evolution of binding energies and peak width (FWHM) of Si and Ca and Ca–Si peak distance during vapor hydration of C_3S.

Time (min)	Peak position (eV)			Ca–Si distance
	Si 2p	Si 2s	Ca $2p_{3/2}$	$\delta_{Ca\ 2p\text{-}Si\ 2p}$
0	101.9 (2.5)	152.9 (3.2)	346.8 (2.7)	245.2
2	101.9 (2.4)	152.9 (3.2)	347.0 (2.7)	245.3
7	102.2 (2.4)	153.2 (3.3)	347.1 (2.6)	245.1
12	102.4 (2.5)	153.3 (3.3)	347.3 (2.6)	245.0
17	102.4 (2.5)	153.3 (3.3)	347.3 (2.6)	244.9
27	102.6 (2.6)	153.5 (3.3)	347.4 (2.5)	245.0
42	102.5 (2.5)	153.4 (3.3)	347.4 (2.5)	244.9
62	102.6 (2.5)	153.5 (3.3)	347.4 (2.5)	244.9
122	102.6 (2.5)	153.4 (3.5)	347.2 (2.5)	244.6
182	102.6 (2.5)	153.4 (3.3)	347.2 (2.5)	244.6

progressive hydration of C_3S results in a shift of the Si 2p and Si 2s peaks to higher binding energies, therefore reducing the value of the distance between the peaks of calcium and silicon. This is due to

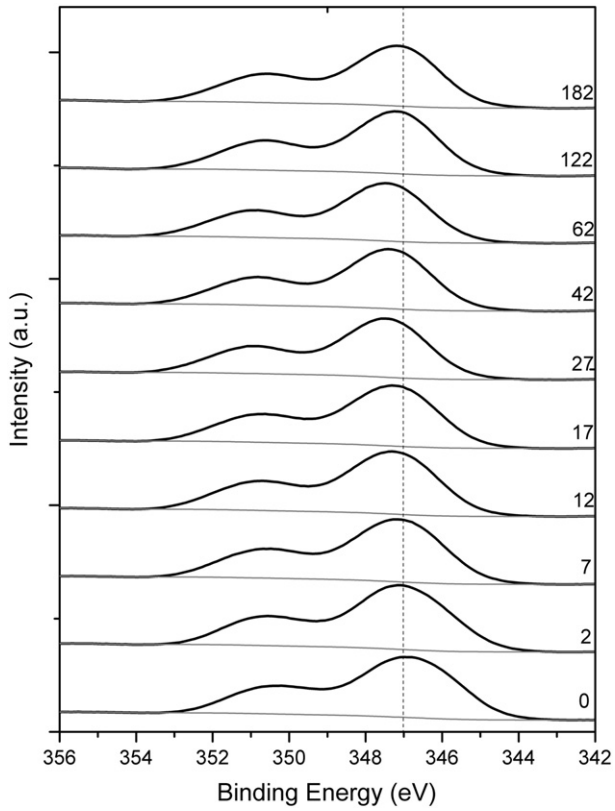

Fig. 2. Calcium spectra (lower and higher energy peaks correspond, respectively, to Ca $2p_{3/2}$ and Ca $2p_{1/2}$ lines) of the C_3S thin film showing the variation of the peaks during the exposure to water vapor.

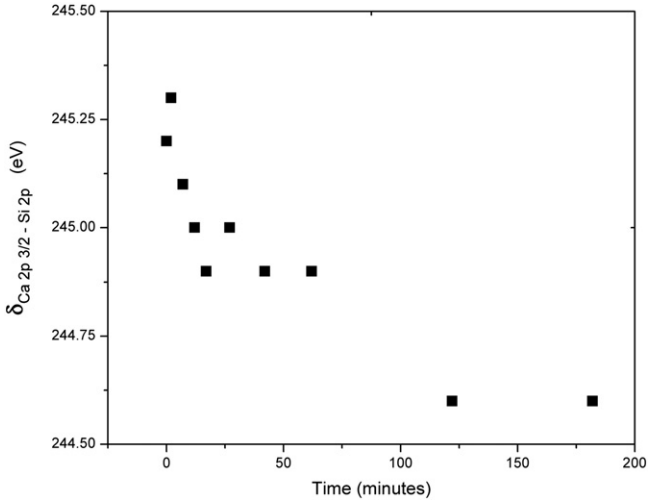

Fig. 3. Evolution of the Ca–Si distance during hydration of C_3S thin films.

the polymerization of the isolated silicate tetrahedra upon formation of C–S–H, and/or carbonation [23]. However, the experimental procedure used in this work (continuous hydration and chemical analysis in situ, without exposing the sample to the atmosphere) prevents potential contamination by external water vapor and/or CO_2 and, therefore, formation of calcium carbonate is not likely to occur during the experiment.

Despite the slight differences in the values of the Ca $2p_{3/2}$ peaks, the reduction of the Ca–Si distance after 3 h of hydration of C_3S found in this work ($\delta_{Ca\ 2p\ 3/2\text{–}Si\ 2p} = 0.6$ eV) is identical to that found by Regourd et al. [6] after 4 h. This strongly suggests that using saturated water vapor conditions (Table 2) does not alter substantially the kinetics of conventional hydration with liquid. The main argument in support of this is that the observed variation of the distance between the peaks of Ca and Si is identical irrespective of the hydration method (Ca binding energy remains constant during hydration but Si varies due to progressive polymerization). Previous work by Regourd et al. [6] has reported a reduction of the Ca–Si distance of 0.6 eV after 4 h of hydration in liquid. We interpret the agreement as indicative that, at least for the materials studied in this work, the kinetics and mechanisms of hydration are essentially the same for liquid or vapor hydration.

The formation of C–S–H on the surface of the C_3S thin film during in situ hydration has also been monitored by a quantitative assessment of the evolution of the molar Ca/Si ratio of the newly formed hydrates. XPS analyses (Table 4) show that the bulk Ca/Si ratio remains constant, confirming the expected isochemical conditions of the experiment. Fast partial hydration and carbonation of the upper few nanometers of the sample (forming, respectively, portlandite

Table 4
Corrected area and bulk Ca/Si ratios.

Age (min)	Corrected area			Ca2p/Si2p	Ca2p/Si2s
	Si 2p	Si 2s	Ca 2p		
0	9442.6	9059.3	32,293.1	3.4	3.6
2	9749.3	9398.7	33,291.2	3.4	3.5
7	9428.8	9122.1	32,109.5	3.4	3.5
12	9422.6	8912.4	31,949.4	3.4	3.6
17	9162.9	8738.6	30,736.3	3.4	3.5
27	8163.1	7911.7	30,736.3	3.8	3.9
42	8014.2	7978.8	29,219.6	3.6	3.7
62	8000.4	7810.0	28,623.0	3.6	3.7
122	8809.1	8780.0	30,593.5	3.5	3.5
182	8302.2	8138.6	30,271.7	3.6	3.7

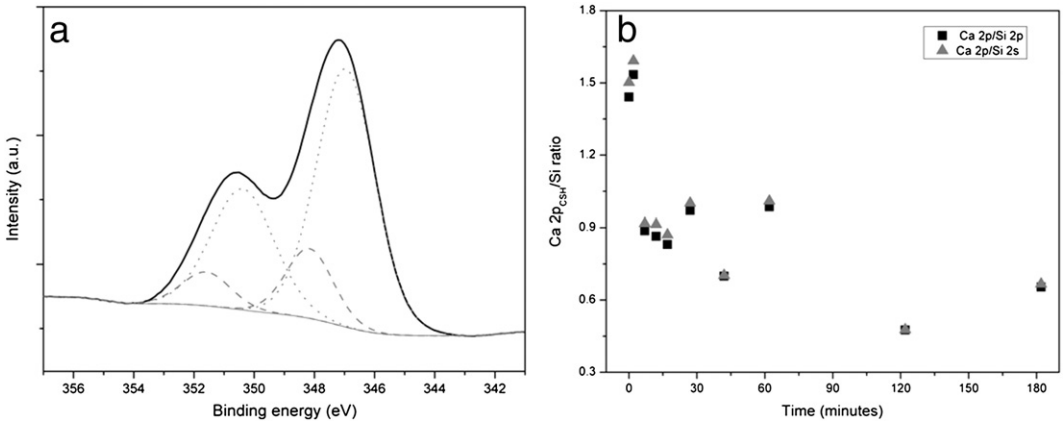

Fig. 4. (a) Deconvolution of the Ca 2p peaks that evidences the calcium carbonate (dotted) and calcium silicate (dashed) contributions; (b): Evolution of the Ca/Si ratio of the C–S–H as a function of hydration time (see text for explanation).

and calcium carbonate) during manipulation under atmospheric conditions may explain the excess Ca content (Ca/Si of about 3.5 *vs.* 3.0 of stoichiometric tricalcium silicate, Table 4).

In order to study the chemical changes during hydration, a deconvolution of the Ca $2p_{1/2}$ and Ca $2p_{3/2}$ peaks has been carried out in order to separate the contributions from calcium carbonates and calcium silicates. Calcium silicates are known to have Ca 2p binding energies slightly higher, about 1.2 eV, than those of calcium carbonates (Fig. 4a). This difference is clearly above the energy resolution limit of the XPS analyses in this work (about 0.1 eV) and, consequently, the contributions of silicates and carbonates to the Ca peaks are clearly distinguishable. When the higher energy components of the Ca 2p peaks are used to correct for the carbonate content, the silicate (hydrate) Ca/Si ratio drops from about 3.5 (uncorrected) to values that decrease from about 1.6 to 0.5, as hydration progresses (Fig. 4b). Although small contributions from portandite and/or unhydrated C_3S cannot be excluded, such low Ca/Si values clearly evidence the presence of C–S–H.

The progressive change of the Ca/Si of the C–S–H indicates structural changes of the silicate hydrates. In fact, the decrease of molar Ca/Si ratio of C–S–H was interpreted to correspond to a progressive polymerization and subsequent increase of chain length, as progressive polymerization of silicate tetrahedra is compositionally equivalent to an increase of SiO_2 content [23,24]. This is consistent with recent views [4] that, after an initial rapid reaction with water, the silicate hydrates undergo a slow dissolution process and subsequent hydration yields to longer chain structures. Results from this work

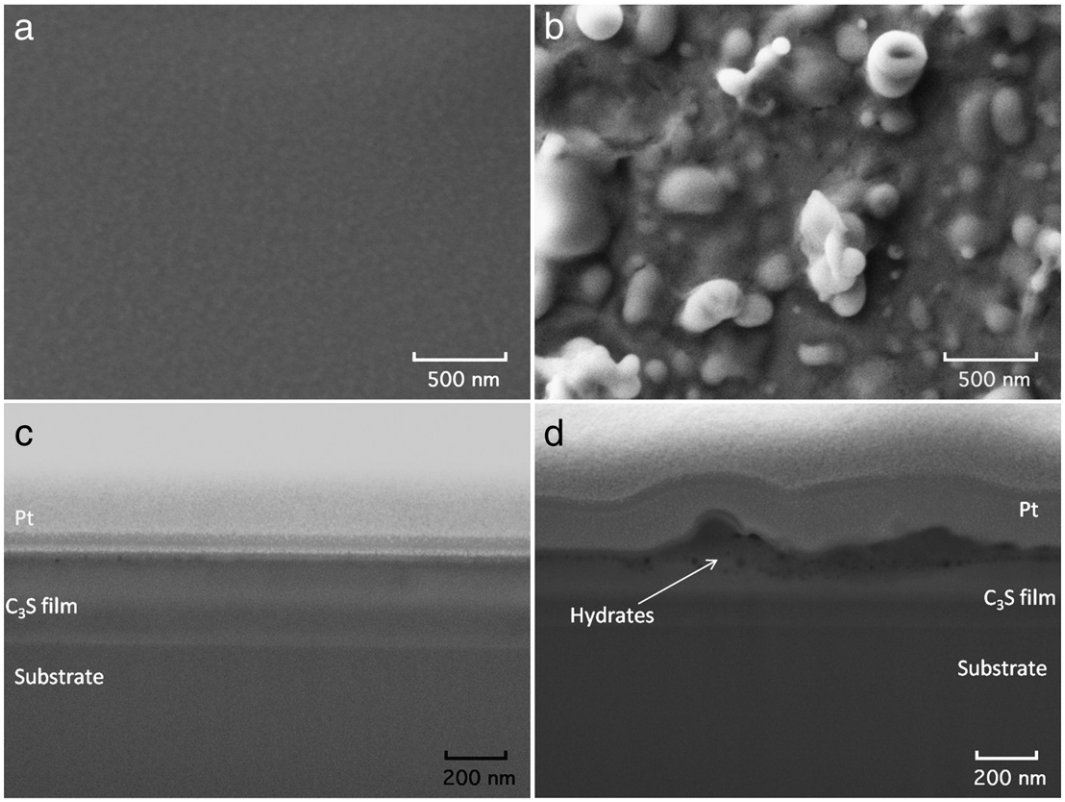

Fig. 5. Scanning electron microscope images of the surface of the C_3S thin films at unhydrated initial conditions (a), and after 182 min of hydration (b). Lower images show a cross section of the unhydrated sample (c) and after exposure to water (d), produced by selective milling with a gallium focused ion beam. Image shows the presence of small hollow bubbles and increasing on the roughness, probably resulting from the formation of C–S–H. Figures show the distinction among the different layers (silicon wafer substrate, C_3S thin film and platinum cover).

strongly suggest that the first precipitate, probably formed by pre-hydration of C_3S under atmospheric conditions, is a jennite-like material, with a Ca/Si ratio of about 1.5, and evolves to a tobermorite-like material at the end of the 3-hour experiment.

Finally, a combined FIB/SEM study has been used to monitor the microstructural changes of the samples. At the beginning of the hydration, the surfaces of the thin films were essentially flat at the nanometric scale, and no significant surface features can be distinguished (Fig. 5a). Roughness due to formation of hydrates increased progressively and at the end of the experiment, small clumps of C–S–H of a few hundreds of nanometers covered all the area exposed to water (Fig. 5b). In order to obtain a cross section view of the sample, and avoid local charging and subsequent defocussing of the FIB, a thin layer of platinum of a few tens of nanometers was deposited on the thin film prior to selective milling. Before exposure to water, C_3S appears as a uniform, flat layer (Fig. 5c); after 182 min of hydration a layer of hydrates, rough and porous, related to the formation of C–S–H is clearly observed (Fig. 5d).

4. Summary and conclusions

Thin films of C_3S were prepared by electron beam evaporation and exposed to water vapor avoiding any contact with air between each stage of hydration and XPS analyses. Samples were found to be partially pre-hydrated and carbonated (during manipulation prior to the experiments); nevertheless, this did not prevent additional hydration.

Monitoring of the position of the Si 2p and Si 2s peaks revealed a shift, as hydration progressed, to higher energies related to silicon polymerization. This is interpreted to evidence the formation of C–S–H. On the other hand, the Ca 2p peak remained essentially centered at the same energy level. Consequently, the distance between the Ca and the Si peaks decreased with time, indicating that the kinetics of early C–S–H formation is not significantly altered when vapor is used instead of liquid water.

The bulk molar Ca/Si ratio (once corrected for carbonate contribution) was found to decrease with hydration time, also indicating a progressive polymerization and increase in chain length of the silicate hydrates formed. Initial Ca/Si values correspond to a jennite-like material, and evolve to a tobermorite-like component after 3 h of exposure to water.

Finally, a scanning electron microscopy study of the evolution of the microstructural changes revealed that, as hydration progressed, the exposed surface was covered with hydrates of a few hundreds of nanometers. In order to obtain a cross section view of the sample and image the progress of the hydrated layers, selective milling with a FIB was carried out. After 3 h of hydration, a rough and porous layer related to the formation of C–S–H was observed.

Acknowledgements

The authors wish to thank Montserrat Domínguez and Trifon Trifonov for technical assistance. V.R. had the financial support of the CUR of the DIUE of the Generalitat de Catalunya. This work is partially funded by grant CTQ2009-12520 from the Spanish Ministry of Science and Innovation. The authors also thank Prof. L. Black for the valuable discussions.

References

[1] S. Garrault-Gauffinet, A. Nonat, Experimental investigation of calcium silicate hydrate (C–S–H) nucleation, J. Cryst. Growth 200 (1999) 565–574.
[2] M.M. Costoya Fernandez, Effect of particle size on the hydration kinetics and microstructural development of tricalcium silicate. PhD Thesis (2008), École Polytechnique Fédérale de Lausanne, Switzerland.
[3] P. Juilland, E. Gallucci, R. Flatt, K. Scrivener, Dissolution theory applied to the induction period in alite hydration, Cem. Concr. Res. 40 (2010) 831–844.
[4] K.L. Scrivener, A. Nonat, Hydration of cementitious materials, present and future, Cem. Concr. Res. 41 (2011) 651–665.
[5] P. Juilland, Early Hydration of Cementitious Systems. PhD Thesis (2009), École Polytechnique Fédérale de Lausanne, Switzerland.
[6] M. Regourd, J.H. Thomassin, P. Baillif, J. Touray, Study of the early hydration of Ca_3SiO_5 by X-ray photoelectron spectrometry, Cem. Concr. Res. 10 (1980) 223–230.
[7] D. Ménétrier, I. Jawed, T.S. Sun, J. Skalny, ESCA and SEM studies on early C_3S hydration, Cem. Concr. Res. 9 (1979) 473–482.
[8] M. Regourd, Microanalytical studies (X-ray photoelectron spectrometry) of surface hydration reactions of cement compounds, Philos. Trans. R. Soc. Lond. A 310 (1983) 85–92.
[9] L. Black, K. Garbev, I. Gee, Surface carbonation of synthetic C–S–H samples: a comparision between fresh and aged C–S–H using X-ray photoelectron spectroscopy, Cem. Concr. Res. 38 (2008) 745–750.
[10] E.M. Gartner, A proposed mechanism for the growth of C–S–H during the hydration of tricalcium silicate, Cem. Concr. Res. 27 (1997) 665–672.
[11] J. Thomas, H. Jennings, J. Chen, Influence of nucleation seeding on the hydration mechanism of tricalcium silicate and cement, J. Phys. Chem. 11 (2009) 4327–4334.
[12] J.W. Bullard, A determination of hydration mechanisms for tricalcium silicate using a kinetic cellular automaton model, J. Am. Ceram. Soc. 91 (2008) 2088–2097.
[13] S. Bishnoi, K. Scrivener, Studying nucleation and growth kinetics of alite hydration using μic, Cem. Concr. Res. 39 (2009) 849–860.
[14] H. Manzano, A. van Duin, S. Yip, M. Buehler, F. Ulm, R. Pellenq, The C–S–H gel formation understood by atomistic simulation methods, XIII International Congress on the Chemistry of Cement, 2011, p. 335.
[15] J.W. Bullard, H.M. Jennings, R.A. Livingston, A. Nonat, G.W. Scherer, J.S. Schwitzer, et al. (2010). Mechanisms of cement hydration. Cem. Concr. Res. 41 (2011), 1208–1223.
[16] J.J. Thomas, J.J. Biernacki, J.W. Bullard, S. Bishnoi, J.S. Dolado, G.W. Scherer, et al., Modeling and simulation of cement hydration kinetics and microstructure development, Cem. Concr. Res. 41 (2011) 1257–1278.
[17] F. Bellmann, D. Damidot, B. Möser, J. Skibsted, Improved evidence for the existence of an intermediate phase during hydration of tricalcium silicate, Cem. Concr. Res. 40 (2010) 875–884.
[18] V. Rheinheimer, N. Veglio, I. Casanova, Production and characterization of clinker thin films as a new tool for nanoscale studies of hydration mechanisms, XIII International Congress on the Chemistry of Cement, 2011, p. 231.
[19] L. Black, A. Stumm, K. Garbev, P. Stemmermann, K.R. Hallam, G.C. Allen, X-ray photoelectron spectroscopy of the cement clinker phases tricalcium silicate and β-dicalcium silicate, Cem. Concr. Res. 33 (2003) 1561–1565.
[20] L. Black, K. Garbev, G. Beuchle, P. Stemmermann, D. Schild, X-ray photoelectron spectroscopic investigation of nanocrystalline calcium silicate hydrates synthesised by reactive milling, Cem. Concr. Res. 36 (2006) 1023–1031.
[21] S. Long, C. Liu, Y. Wu, ESCA study on the early C_3S hydration in NaOH solution and pure water, Cem. Concr. Res. 28 (1998) 245–249.
[22] L. Black, K. Garbev, P. Stemmermann, K.R. Hallam, G.C. Allen, Characterisation of crystalline C–S–H phases by X-ray photoelectron spectroscopy, Cem. Concr. Res. 33 (2003) 899–911.
[23] M.Y.A. Mollah, T.R. Hess, Y.-N. Tsai, D.L. Cocke, An FTIR and XPS investigation of the effects of carbonation on the solidification/stabilization of cement based systems—portland type V with zinc, Cem. Concr. Res. 23 (1993) 773–784.
[24] H.F.W. Taylor, Proposed structure for calcium silicate hydrate gel, J. Am. Ceram. Soc. 69 (1986) 464–467.